RSC Advances

PAPER

View Article Online
View Journal | View Issue

Cite this: *RSC Adv.*, 2016, **6**, 83366

Molecular weight effects of PEG on the crystal structure and photocatalytic activities of PEG-capped TiO_2 nanoparticles

Meizhou Zhang, Jinfeng Lei, Yifeng Shi, Lina Zhang, Youxin Ye, Defu Li* and Changdao Mu*

Polyethylene glycol (PEG) was used as stabilizer to prepare water-soluble anatase titanium dioxide (TiO_2). The molecular weight effects of PEG on the crystal structure and photocatalytic activities of PEG-capped TiO_2 nanoparticles were systematically studied. The results show that the steric hindrance effect of PEG molecular chains will hinder the PEG molecules from being tied to the surface of TiO_2, resulting in the decrease of PEG molecules capped on the surface of TiO_2 with the growth of PEG molecular chains. It is significant that PEG can effectively promote the dispersion of TiO_2 nanoparticles in water, which becomes better and better with the increase of molecular weight of PEG. Moreover, the PEG-capped TiO_2 aqueous solutions can keep stable for more than two months. PEG cannot influence the crystal type and size of TiO_2, which can be well controlled by the introduction of HCl in the reaction system. The photocatalytic activity of PEG-capped TiO_2 was evaluated by monitoring the degradation of methyl orange, which is better than that of commercial P25 TiO_2 mainly due to the good dispersion in water. However, PEG molecular chains are detrimental to the transfer of photogenerated electrons and reactive oxygen species while the increasing dispersion in water with the increase of PEG molecular weight can increase the photocatalytic activity of TiO_2. As a result, PEG400 capped TiO_2 presents the best photocatalytic activity while PEG2000 capped TiO_2 exhibits the worst photocatalytic activity. The photocatalytic activity begins to increase when the molecular weight of PEG is larger than 2000.

Received 19th May 2016
Accepted 29th August 2016

DOI: 10.1039/c6ra12988a

www.rsc.org/advances

1. Introduction

Titanium dioxide (TiO_2), one of the most promising photocatalysts, has been widely investigated for decades since Fujishima discovered the photocatalytic splitting of water on TiO_2 electrodes.[1–4] TiO_2 nanoparticles (NPs) have multiple advantages such as good structural stability, abundance, non-toxicity and low cost.[5–7] Hence, TiO_2 NPs have been used in many areas for instance solar energy conversion,[8–10] photocatalytic self-cleaning,[11–15] sensors[16–18] and photochromic devices.[19,20]

TiO_2 has three crystallographic phases: anatase, brookite and rutile.[21] Among them, the anatase TiO_2 has been confirmed to have excellent photoactivity and optoelectronic properties.[22,23] However, the high purity anatase TiO_2 is difficult to be prepared by traditional methods, because that the hydrolytic process of many traditional methods for the preparation of TiO_2 is hard to be controlled at room temperature and titanium alkoxides are sensitive to moisture.[24] Nowadays, new routes have been developed to prepare high quality anatase TiO_2 NPs by using an organic media to reduce the sensitivity of precursor to moisture.[25–27] However, the surface of produced TiO_2 NPs is often hydrophobic due to the hydrophobicity of capped organic media like oleic acid, which limits the applications of TiO_2 NPs since the most applications are carried out in aqueous solution.[24] Recently, Wang and co-workers[24] have successfully prepared water-soluble anatase TiO_2 NPs using ethylene glycol as a surfactant. Yan and co-workers[28] have reported a new and facile route for the controllable synthesis of water-soluble anatase TiO_2 NPs using polyethylene glycol 400 (PEG400) as a solvent and a stabilizer, with phases well controlled by introduction of HCl in the reaction system. The results indicated that PEG was an effective media for the preparation of water-soluble anatase TiO_2 NPs. It is known that the capped surfactant should impact the surface activity of TiO_2 NPs, which has been thought to be correlated with its photovoltaic and photocatalytic properties.[24] However, to the best of our knowledge, only ethylene glycol and PEG400 have been used as stabilizers to prepare water-soluble anatase TiO_2 NPs. The effects of molecular weight of PEG on the structure and photocatalytic activity of TiO_2 NPs have not attracted enough attention, which has not been discussed in detail.

In this work, a series of PEG with different molecular weight were used as stabilizers to prepare water-soluble TiO_2 NPs. The

Department of Pharmaceutics and Bioengineering, School of Chemical Engineering, Sichuan University, Chengdu 610065, China. E-mail: lidefu@scu.edu.cn; cdmu@scu.edu.cn

anatase phase of TiO_2 was controlled by introduction of HCl in the reaction system. Then the crystal structures and physicochemical properties of the PEG-capped TiO_2 NPs were investigated. The photocatalytic activities of the TiO_2 NPs were evaluated by monitoring the degradation of methylene blue (MB) and methyl orange (MO). Our aim is to understand the effects of molecular weight of PEG on the crystal structure and photocatalytic activities of PEG-capped TiO_2 nanoparticles.

2. Experimental section

2.1 Materials

Titanium butoxide (≥99.0%) and polyethylene glycol (PEG) were purchased from Aladdin Industrial Corporation (Shanghai, China). Hydrochloric acid (HCl, 36.0–38.0%) was purchased from Kelong Chemical Reagent Company (Chengdu, China). Commercial P25 TiO_2 powder was purchased from Sigma-Aldrich Corporation.

2.2 Preparation of the PEG-capped TiO_2 NPs

TiO_2 NPs capped by PEG with different molecular weight were prepared according to previous method with a slight modification.[28] 3 mL of titanium butoxide was mixed with 6 g of PEG under magnetic stirring at 65 °C to form a white titanium alkoxide complex. Then, 1 mL of HCl was dropped into the titanium alkoxide complex. The formed transparent slight yellow solution was then transferred to a stainless poly (tetra fluoroethylene) (Teflon)-lined autoclave (50 mL) and heated in a vacuum drying oven at 150 °C for 5 h. The tawny TiO_2 products were separated by high-speed centrifugation (10 000 rpm), thoroughly washed with hot ethanol for 2–3 times and dried in the vacuum drying oven at 50 °C for 24 h. 5 types of PEG with molecular weight of 400, 2000, 4000, 6000 and 10 000 were used to prepare TiO_2 NPs. The corresponding resulting products were named as TP400, TP2000, TP4000, TP6000 and TP10000, respectively.

2.3 Characterization of the PEG-capped TiO_2 NPs

The particle size of TiO_2 NPs in aqueous solution was measured using a Malvern Zetasizer Nano – ZS ZEN3600 instrument at a detection angle of 90° at 25 °C. The concentration of TiO_2 NPs aqueous solution was 2 g L^{-1}. The mean particle sizes were obtained in the cumulant mode using the built-in Malvern software. The crystal structures of the TiO_2 NPs were identified by an 18 kW X-ray diffractometer (X'Pert Pro, Philips, Almelo, Netherlands) with a fixed CuKα radiation (λ = 1.54 Å). The scanning range of the diffraction angle (2θ) was from 10° to 80° with a rate of 2° min^{-1}. The morphology and microstructure of the TiO_2 NPs were characterized by transmission electron microscopy (TEM) (JEM-2100, JEOL, Japan) and scanning electron microscopy (SEM) (JSM-7500F, JEOL, Japan). Thermogravimetric analysis (TGA) of the samples was carried out on a NETZSCH thermal analyzer (TG209F1, NETZSCH, Germany). The samples were dried in a vacuum drying oven at 105 °C for 24 h before the test. The measurements were running from 50 °C to 700 °C at a heating rate of 10 °C min^{-1} and under nitrogen atmosphere to avoid thermo-oxidative reactions.

2.4 Photocatalytic activity evaluation of the PEG-capped TiO_2 NPs

The photocatalytic activities of the PEG-capped TiO_2 NPs were evaluated by monitoring the degradation of methylene blue (MB) and methyl orange (MO). 30 mg of TiO_2 NPs was suspended in 15 mL aqueous solution of MB or MO (10 mg L^{-1}) to obtain the reaction slurry. The slurries were stirred for 6 h in the dark to assure the establishment of an adsorption–desorption equilibrium. Then, the slurries were irradiated by a 90 W UV lamp (maximum emission at 302 nm). The photocatalytic degradation of MB was examined by measuring its absorbance at 664 nm every 30 minutes. The photocatalytic degradation of MO was examined by measuring its absorbance at 464 nm every 30 minutes. The measurements were carried out for five times and the mean values were used.

2.5 Statistical analyses

The SPSS version 17.0 software was used for statistical analysis of experimental data. Data were assessed with one-way analysis of variance (ANOVA) by using Duncan's multiple range test. A value of $p < 0.05$ was considered to be significant.

3. Results and discussion

3.1 Preparation and characterization of the PEG-capped TiO_2 NPs

The photographs of the PEG-capped TiO_2 NPs aqueous solutions are presented in Fig. 1. It can be seen that the series of TiO_2 NPs capped by PEG with different molecular weight all have good dispersion in water. Furthermore, we found that the PEG-capped TiO_2 NPs aqueous solutions can maintain stable for more than two months without obvious precipitation. It is worth noting that the transparency of the TiO_2 NPs aqueous solutions is increasing from TP400 to TP10000. The result indicates that the dispersion of TiO_2 NPs in water is getting better with the increase of molecular weight of PEG. To further understand the water solubility of PEG-capped TiO_2 NPs, the particle sizes of the PEG-capped TiO_2 NPs in aqueous solutions were measured and showed in Table 1. It is obvious that the particle size of TiO_2 NPs decreases from 76.2 to 49.2 nm with the growth of PEG molecular chains. The result is agreed with previous works that PEG can promote the dispersion of TiO_2

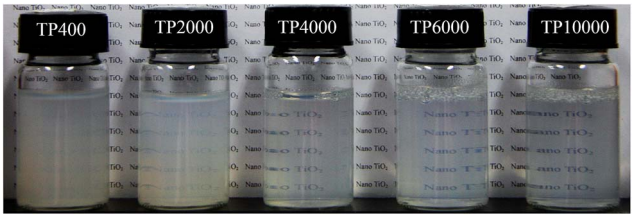

Fig. 1 Photographs of the PEG-capped TiO_2 NPs aqueous solutions.

Table 1 Particle sizes of the PEG-capped TiO_2 NPs in aqueous solutions

Samples	TP400	TP2000	TP4000	TP6000	TP10000
Particle size (nm)	76.2	68.6	60.9	56.3	49.2

NPs in water.[28] Furthermore, the dispersion of TiO_2 NPs in water can become better when capped by PEG with longer molecular chain.

To study the crystallographic phases of as-prepared PEG-capped TiO_2 NPs, the typical XRD patterns of the PEG-capped TiO_2 NPs were measured and showed in Fig. 2. There is almost no difference among the five samples. They exhibit distinctive characteristic peaks at 2 theta 25.2°, 37.8°, 47.8°, 53.9°, 62.2° and 69.7°, corresponding to the anatase phase planes of (101), (004), (200), (105), (204) and (116) according to JCPDS card no. 21-1272.[29] The result indicates that the produced PEG-capped TiO_2 NPs are anatase phase. Yan and co-workers have successfully prepared water-soluble anatase TiO_2 NPs under mild solution conditions using PEG400 as a stabilizer and HCl as a phase controlling reagent. The results showed that the amount of concentrated HCl in the reaction system was found to have a strong influence on the TiO_2 crystal phases. For the low HCl content, the pure anatase phase could be produced.[28] In our work, PEG with different molecular weight were used as stabilizers while the low HCl content was selected. The water-soluble anatase TiO_2 NPs were successfully prepared too. The result indicates that the molecular weight of PEG has no influence on the crystal structures of the TiO_2 NPs, which can be controlled by the introduction of HCl in the reaction system.

The morphology and microstructure of the PEG-capped TiO_2 NPs were characterized by TEM and SEM to further study the crystallographic phases of as-prepared PEG-capped TiO_2 NPs. Fig. 3 shows the TEM images of the PEG-capped TiO_2 NPs. It can be observed that the TiO_2 NPs exhibit almost spheroidal shapes with the average grain sizes in the range of 5–10 nm, which is consistent with the shapes of anatase TiO_2 reported in previous works.[12] Note that the grain size of the TiO_2 in Fig. 3 is much smaller than that in aqueous solutions (Table 1). Moreover, the grain sizes of the TiO_2 are basically the same while the particle sizes of TiO_2 NPs in water decrease as the growth of PEG

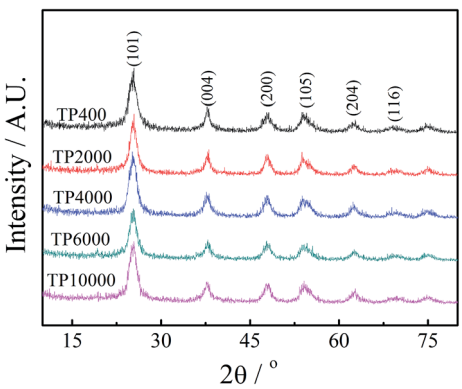

Fig. 2 XRD patterns of the PEG-capped TiO_2 NPs.

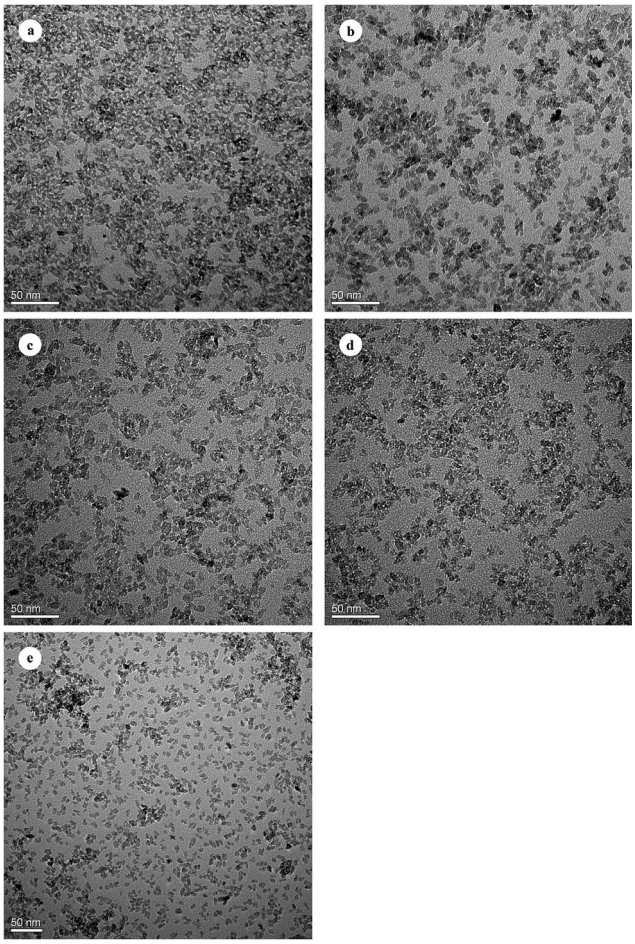

Fig. 3 TEM images of the PEG-capped TiO_2 NPs. (a) TP400, (b) TP2000, (c) TP4000, (d) TP6000 and (e) TP10000.

molecular chains. The results indicate that TiO_2 is present in the form of aggregates in water. PEG can facilitate the dispersion of TiO_2 NPs in water, but cannot influence the crystal types and size of TiO_2 NPs. Fig. 4 shows the SEM images of the PEG-capped TiO_2 NPs. As seen from Fig. 4, the samples present spherical shapes, which is consistent with the results gotten from TEM images. However, the morphology of TiO_2 NPs gradually becomes unclear with the increase of the molecular weight of PEG. The reason may be that PEG capped on the surface of TiO_2 NPs with high molecular weight can make TiO_2 NPs present the morphology of polymers.

TGA was used to evaluate whether PEG was capped on the surface of TiO_2 NPs according to the published method.[30] Fig. 5 shows the TGA and DTG curves of the PEG-capped TiO_2 NPs. The weight loss of the PEG-capped TiO_2 NPs at 700 °C and the ratio of weight loss to molecular weight of PEG were calculated and showed in Table 2. It is found that the weight losses for TP400, TP2000, TP4000, TP6000 and TP10000 at 700 °C are 24.70, 17.31, 18.03, 23.57 and 27.61 wt%, respectively. The weight losses are mainly attributed to the decomposition of organic groups on the surface of TiO_2, which verifies that PEG has been successfully capped on the surface of TiO_2 NPs. Table 2 shows that the weight losses of TiO_2 NPs at 700 °C are

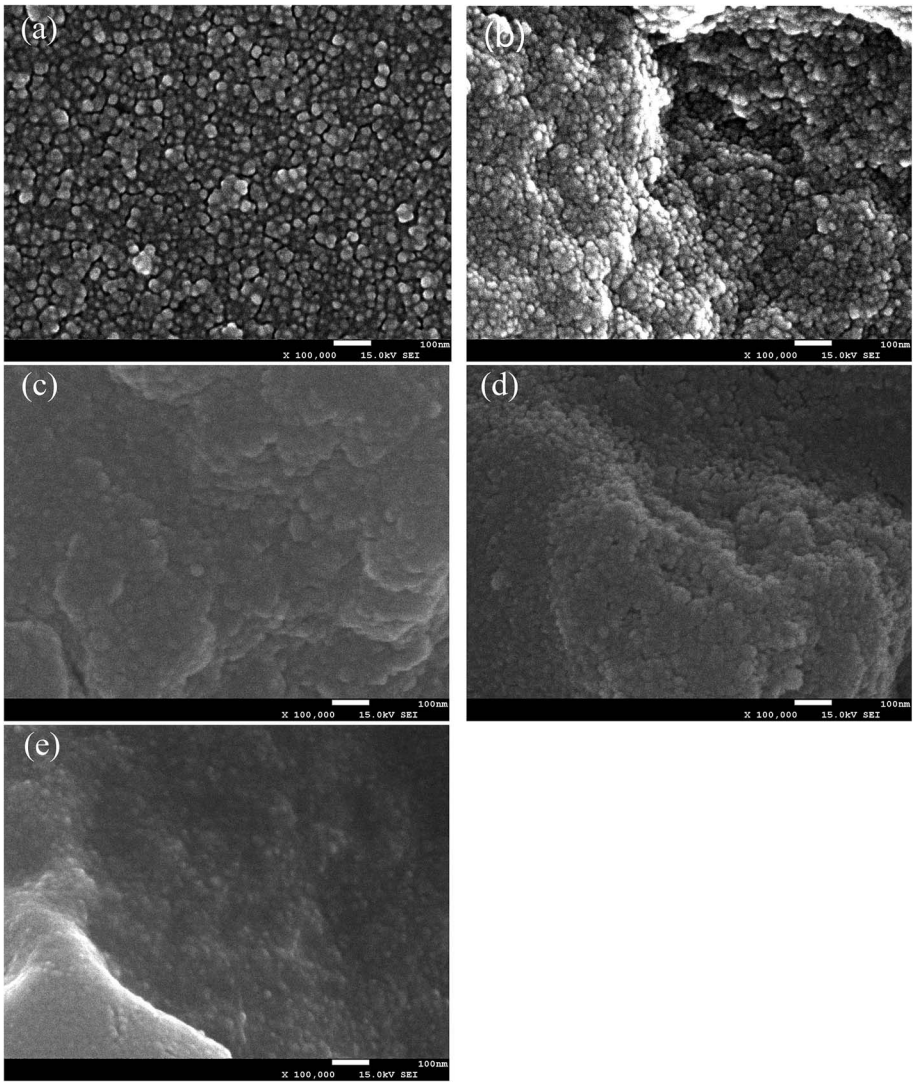

Fig. 4 SEM images of the PEG-capped TiO_2 NPs. (a) TP400, (b) TP2000, (c) TP4000, (d) TP6000 and (e) TP10000.

irregular. However, it is interesting that the ratio of weight loss to molecular weight of PEG is decreasing with the increase of molecular weight of PEG. The result indicates that the number of PEG molecules capped on the surface of TiO_2 is reduced with the growth of PEG molecular chains. The reason may be that the growth of PEG molecular chain leads to the increase of steric hindrance to result in the decrease of reaction site for PEG molecules.

3.2 Photocatalytic activity of the PEG-capped TiO_2 NPs

The photocatalytic activities of the PEG-capped TiO_2 NPs were evaluated by monitoring the degradation of methylene blue (MB) and methyl orange (MO). Fig. 6 shows the photocatalytic degradation of MB in the presence of PEG-capped TiO_2 under UV light irradiation and the corresponding photographs *versus* irradiation time. It shows that the degradation of MB takes place induced by PEG-capped TiO_2 NPs. The reaction slurry of TP400 becomes colorless after the UV-irradiation for 30 minutes. However, it is interesting that the color begins to recover in 150 minutes. The same phenomenon can be observed for TP2000. The phenomenon of reversible color change of MB has been reported by previous works, which is attributed to the reduction–oxidation behavior of MB.[31,32] The oxidized form of MB presents blue and the reduced form is colorless. The oxidation–reduction potential of MB is lower than the conduction band edge of TP400 and TP2000. Hence, the photogenerated electrons transferred from TP400 and TP2000 to the MB molecules reduce the MB molecules from blue to the colorless state. However, the reversible color phenomenon cannot be observed for TP4000, TP6000 and TP10000. It may be because that the conduction band edge of TP4000, TP6000 and TP10000 is lower than the oxidation–reduction potential of MB.

This reversible color phenomenon of MB is very interesting, but is not convenient for the present purpose. To solve this problem, methyl orange (MO) was used as a probe to evaluate the photocatalytic activities of the PEG-capped TiO_2 NPs again. Fig. 7 shows the photocatalytic degradation of MO in the presence of PEG-capped TiO_2 under UV light irradiation and the

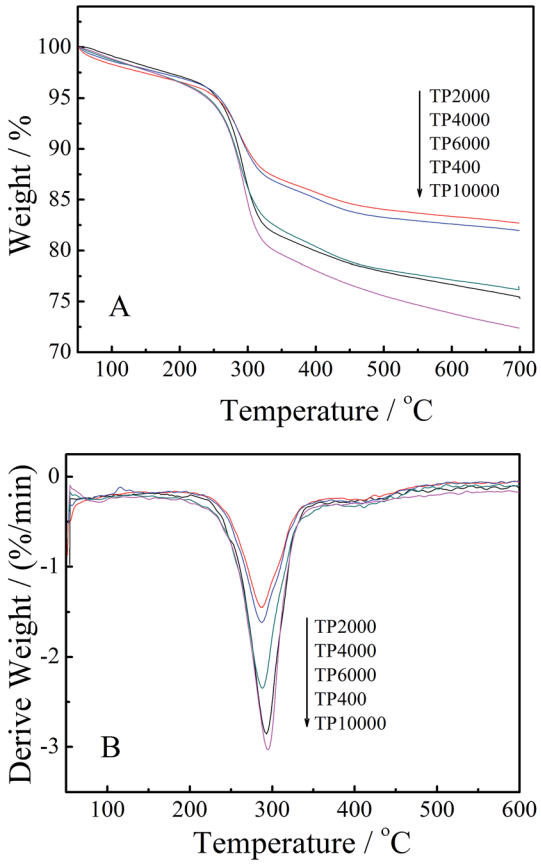

Fig. 5 TGA (A) and DTG (B) curves of the PEG-capped TiO_2 NPs.

Table 2 Weight loss of the PEG-capped TiO_2 NPs at 700 °C and the ratio of weight loss to molecular weight of PEG

Samples	Weight loss (%)	Weight loss/molecular weight of PEG
TP400	24.70	0.062
TP2000	17.31	0.009
TP4000	18.03	0.005
TP6000	23.57	0.004
TP10000	27.61	0.003

corresponding photographs *versus* irradiation time. It is obvious that the photocatalytic activity of all the PEG-capped TiO_2 NPs is better than that of commercial P25 TiO_2. The result illustrates that the presence of PEG on the surface of TiO_2 NPs can increase the photocatalytic activity of TiO_2 mainly due to the resulting good dispersion in aqueous solution. The same results have been reported by previous work.[28] Fig. 7 shows that TP400 presents the best photocatalytic activity and MO can be absolutely degraded in about 60 minutes. TP2000 exhibits the worst photocatalytic activity and it needs 300 minutes to completely degrade MO. The photocatalytic activity of the PEG-capped TiO_2 NPs begins to increase with the growth of PEG molecular chain when the molecular weight of PEG is larger than 2000.

Fig. 8 shows the tentative photodegradation mechanism diagram of MB and MO on the surface of PEG-capped TiO_2 NPs. The electrons of TiO_2 NPs are stimulated under the UV-irradiation and then transfer from the valence band (VB) to the conduction band (CB).[33] Then the photogenerated electrons are captured directly by O_2 and formed superoxide anion (O^{2-}). Meanwhile, the valence band hole can oxidize water or OH^- to form $^{\bullet}OH$ radicals.[34] These reactive oxygen species would decompose organic dye to CO_2 and water. The results in Fig. 7 show that the PEG molecular chains capped on the surface of TiO_2 are detrimental to the transfer of photogenerated electrons and reactive oxygen species. Previous works have supposed that the strongly bonded surfactant should passivate the surface activity of TiO_2 NPs, resulting in the decrease of the photovoltaic and photocatalytic properties.[35] So the TP400 capped by PEG with the shortest molecular chain presents the best photocatalytic activity. But then, the photocatalytic activity of TiO_2 NPs is not only dependent on the photogenerated electrons, but also dependent on the particle size and surface area.[32] The smaller the particles, the larger will be its specific surface area and the higher the photocatalytic activity. So the photocatalytic activity of the PEG-capped TiO_2 NPs begins to increase when the molecular weight of PEG is larger than 2000, which is mainly due to the increasing dispersion of the PEG-capped TiO_2 NPs in aqueous solutions.

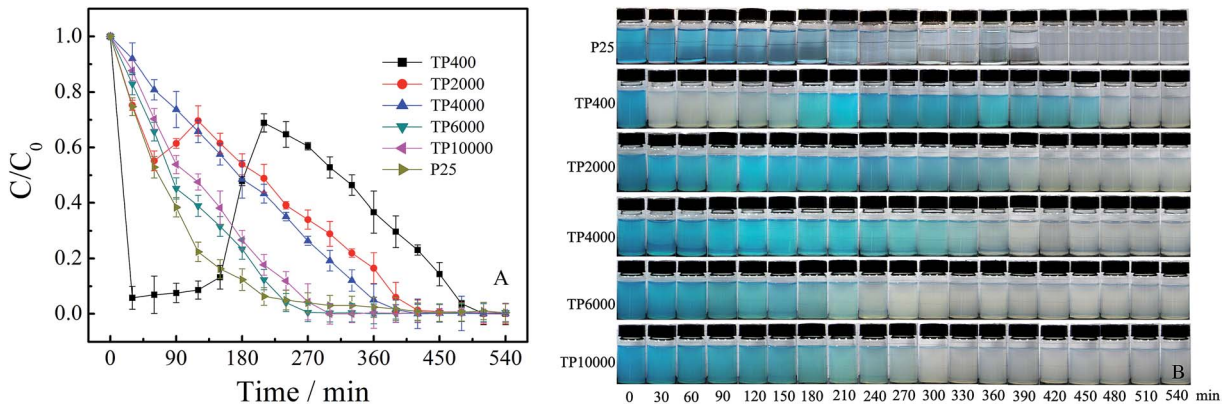

Fig. 6 Photocatalytic degradation of MB in the presence of PEG-capped TiO_2 under UV light irradiation (A) and the corresponding photographs *versus* irradiation time (B).

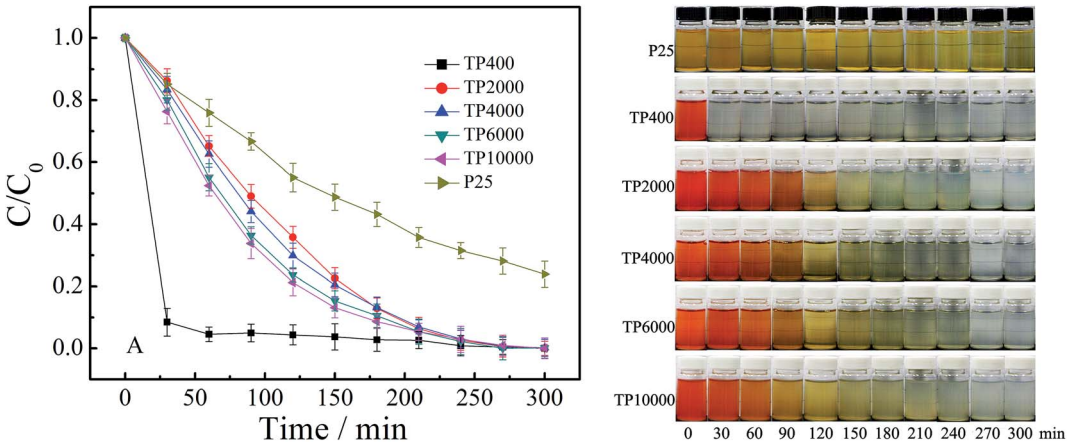

Fig. 7 Photocatalytic degradation of MO in the presence of PEG-capped TiO_2 under UV light irradiation (A) and the corresponding photographs *versus* irradiation time (B).

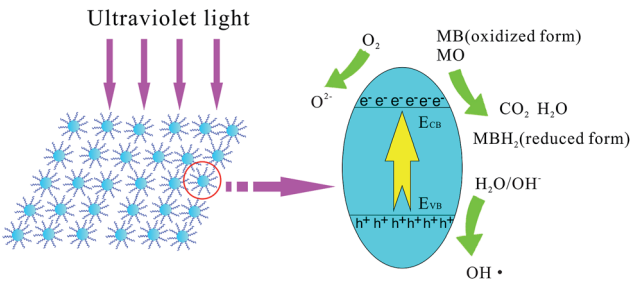

Fig. 8 Tentative photodegradation mechanism diagram of MB and MO on the surface of PEG-capped TiO_2 NPs.

4. Conclusions

PEG-capped TiO_2 nanoparticles have good dispersion in water, which becomes better and better with the increase of molecular weight of PEG. Moreover, the PEG-capped TiO_2 aqueous solutions can maintain stable for more than two months without obvious precipitation. PEG cannot influence the crystal type and size of TiO_2, which can be well controlled as anatase phase by introduction of HCl in the reaction system. PEG molecular chains will hinder the PEG molecules from being tied to the surface of TiO_2, resulting in the decrease of PEG molecules capped on the surface of TiO_2 with the increase of molecular weight of PEG. Moreover, the PEG molecular chains are detrimental to the transfer of photogenerated electrons and reactive oxygen species. So the TiO_2 capped by PEG with the shortest molecular chain presents the best photocatalytic activity. But then, the increasing dispersion of PEG-capped TiO_2 in water with the increase of PEG molecular weight can increase the photocatalytic activity of TiO_2. So the photocatalytic activity of the PEG-capped TiO_2 begins to increase when the molecular weight of PEG is larger than 2000.

Acknowledgements

This study was supported by the National Natural Science Foundation of China (NNSF) (21276166) and Fundamental Research Funds for the Central Universities of China (2015SCU04A34).

References

1 A. Fujishima and K. Honda, *Nature*, 1972, **238**, 37–38.
2 R. Asahi, T. Morikawa, T. Ohwaki, K. Aoki and Y. Taga, *Science*, 2001, **293**, 269–271.
3 M. Anpo and M. Takeuchi, *J. Catal.*, 2003, **216**, 505–516.
4 J. Choi, H. Park and M. R. Hoffmann, *J. Phys. Chem. C*, 2010, **114**, 783–792.
5 K. Nakata and A. Fujishima, *J. Photochem. Photobiol., C*, 2012, **13**, 169–189.
6 K. Nakata, T. Ochiai, T. Murakami and A. Fujishima, *Electrochim. Acta*, 2012, **84**, 103–111.
7 R. Ren, Z. H. Wen, S. M. Cui, Y. Hou, X. R. Guo and J. H. Chen, *Sci. Rep.*, 2015, **5**, 10714.
8 A. Hagfeld and M. Gratzel, *Chem. Rev.*, 1995, **95**, 49–68.
9 S. Nakade, M. Matsuda, S. Kambe, Y. Saito, T. Kitamura, T. Sakata, Y. Wada, H. Mori and S. Yanagida, *J. Phys. Chem. B*, 2002, **106**, 10004–10010.
10 B. O'Regan and M. Grätzel, *Nature*, 1991, **353**, 737–740.
11 S. Banerjee, D. D. Dionysiou and S. C. Pillai, *Appl. Catal., B*, 2015, **176–177**, 396–428.
12 K. C. Li, J. G. Peng, M. Z. Zhang, J. Heng, D. F. Li and C. D. Mu, *Colloids Surf., A*, 2015, **470**, 92–99.
13 W. G. Shen, C. Zhang, Q. Li, W. S. Zhang, L. Cao and J. Y. Ye, *J. Cleaner Prod.*, 2015, **87**, 762–765.
14 E. González, A. Bonnefond, M. Barrado, A. M. C. Barrasa, J. M. Asua and J. R. Leiza, *Chem. Eng. J.*, 2015, **281**, 209–217.
15 F. R. Wang, G. Q. Zhang, Z. Zhao, H. Q. Tan, W. X. Yu, X. M. Zhang and Z. C. Sun, *RSC Adv.*, 2015, **5**, 103752–103759.
16 N. L. Wu, S. Y. Wang and I. A. Rusakova, *Science*, 1999, **285**, 1375–1377.
17 Y. F. Zhu, J. J. Shi, Z. Y. Zhang, C. Zhang and X. R. Zhang, *Anal. Chem.*, 2002, **74**, 120–124.
18 M. Faisal, A. A. Ismail, F. A. Harraz, H. Bouzid, S. A. Al-Sayari and A. Al-Hajry, *Chem. Eng. J.*, 2014, **243**, 509–516.

19 K. I. Iuchi, Y. Ohko, T. Tatsuma and A. Fujishima, *Chem. Mater.*, 2004, **16**, 1165–1167.
20 M. Biancardo, R. Argazzi and C. A. Bignozzi, *Inorg. Chem. Commun.*, 2005, **44**, 9619–9621.
21 A. Wells, *Structural Inorganic Chemistry*, 1975, vol. 4, pp. 377–413.
22 U. Diebold, *Surf. Sci. Rep.*, 2003, **48**, 53–229.
23 K. Nagaveni, G. Sivalingam, M. S. Hegde and G. Madras, *Appl. Catal., B*, 2004, **48**, 83–93.
24 P. Wang, D. J. Wang, H. Y. Li, T. F. Xie, H. Z. Wang and Z. L. Du, *J. Colloid Interface Sci.*, 2007, **314**, 337–340.
25 P. D. Cozzoli, A. Kornowski and H. Weller, *J. Am. Chem. Soc.*, 2003, **125**, 14539–14548.
26 Z. H. Zhang, X. H. Zhong, S. H. Liu, D. F. Li and M. Y. Han, *Angew. Chem., Int. Ed.*, 2005, **44**, 3466–3470.
27 X. L. Li, Q. Peng, J. X. Yi, X. Wang and Y. Li, *Chem. Eur. J.*, 2006, **12**, 2383–2391.
28 X. M. Yan, D. Y. Pan, Z. Li, Y. Y. Liu, J. C. Zhang, G. Xu and M. H. Wu, *Mater. Lett.*, 2010, **64**, 1833–1835.
29 S. Chu, L. L. Luo, J. C. Yang, F. Kong, S. Luo, Y. Wang and Z. G. Zou, *Appl. Surf. Sci.*, 2012, **258**, 9664–9667.
30 Y. W. Wang, F. F. Duo, S. Q. Peng, F. L. Jia and C. M. Fan, *J. Colloid Interface Sci.*, 2014, **430**, 31–39.
31 K. Doushita and T. Kawahara, *J. Sol-Gel Sci. Technol.*, 2001, **22**, 91–98.
32 F. Sayılkan, M. Asiltürk, S. Erdemoğlu, M. Akarsu, H. Sayılkan, M. Erdemoğlu and E. Arpaç, *Mater. Lett.*, 2006, **60**, 230–235.
33 Y. C. Li, Y. Q. Wang, J. H. Kong, H. X. Jia and Z. S. Wang, *Appl. Surf. Sci.*, 2015, **344**, 176–180.
34 L. Zeng, Z. Lu, J. Yang, M. H. Li, W. L. Song and C. S. Xie, *Appl. Catal., B*, 2015, **166–167**, 1–8.
35 T. L. Thompson and J. T. Yates, *Chem. Rev.*, 2006, **106**, 4428–4453.

